Gaussian Synapse Networks for Hyperspectral Image Segmentation

J. L. Crespo, R. J. Duro and F. López-Peña

Grupo de Sistemas Autónomos, Universidade da Coruña, Spain
crespo@cdf.udc.es, richard@udc.es, flop@udc.es

Abstract. In this work we have made use of a new type of network with non linear synapses, Gaussian Synapse Networks, for the segmentation of hyperspectral images. These structures were trained using the GSBP algorithm and present two main advantages with respect to other, more traditional, approaches. On one hand, through the intrinsic filtering ability of the synapses, they permit concentrating on what is relevant in the spectra and automatically discard what is not. On the other, the networks are structurally adapted to the problem as superfluous synapses and/or nodes are implicitly eliminated by the training procedure.

1 Introduction

Remote land observation has been going on for decades. Until recently, most of these observations were carried out through multispectral imagery. Due to limited number of bands of these images, that is, their low spectral resolution, similar land covers could not be differentiated, thus reducing their applicability. To overcome these limitations, imaging spectrometry was developed to acquire images with high spectral resolution. This type of spectrometry is usually called hyperspectral imaging. Hyperspectral images can be defined as those that cover the 400-2500 nm (near infrared to visible) wavelength band with a number of samples between 50 and 250. This corresponds to a sampling of wavelengths in the order of 0.01 micrometers, which is adequate to describe the spectral variability of most surfaces in this wavelength range. This type of technology is relatively new, but we can find a number of commercially available hyperspectral sensors. Staenz [1] lists 14 current instruments with more than 100 spectral bands in this wavelength range. These sensors are mounted on specially prepared airplanes and, depending of the conditions of flight, a hyperspectral pixel can correspond to an area between 15 and 300 square meters, approximately.

The main advantage of hyperspectral imaging with respect to classical remote sensing is the large amount of information it provides. Unfortunately, like in all remote sensing techniques, it still presents the problem of removing the effects induced by whatever is present between the target and the sensor, that is, the atmosphere.

The influence of the atmosphere may be divided into two groups of effects: Those that are spatially and temporally constant and those that are not. In the first category we can include the absorption and scattering by CO_2, N_2, CH_4 and O_2 (well mixed in the atmosphere), and in the second, those elements that could vary in certain circumstances (like water vapor, ozone and aerosols –dust, water droplets and haze-). To eliminate such influences, it is necessary to make a transformation of the measured radiances into reflectances [2]. There are two possible ways to obtain such a transformation: by radiative transfer models or using ground truth. The use of radiative transfer models is not satisfactory in most cases as the necessary information on atmospheric conditions is seldom available, consequently the reflectance accuracy is limited by the simulation of the atmosphere which turns out to be a hard and resource consuming task due to the combined effects enumerated earlier. As an example of this problem, Goetz [3] assumes that surface reflectance varies linearly with wavelength in the spectral range from approximately 1.0 micrometers to 1.3 micrometers. They develop an estimate of surface reflectance and atmospheric water vapor using reflectance data at high spectral resolution (of the order of 10 nm). If we look into their discussion on the physics underlying this problem and the motivation for addressing it, we can see how complex it becomes. Therefore the procedure used (regression by linear least squares) was very time consuming. Gao and Goetz [3] state that retrievals of water vapor for 20,000 spectra from the Advanced Visible Infrared Imaging Spectrometer (AVIRIS) [4] require 200 minutes of processing on their computers.

The ground truth approach measures the reflectance at selected ground control points at the time of the remotely sensed image. Alternatively it can provide in situ classifications of some targets instead of measuring their reflectances [5]. This last approach has been used in this study.

From the data processing viewpoint and although theoretically the use of hyperspectral images should increase our abilities to identify various materials, the classification methods used for multispectral images are not adequate and the results are not as good as desired. This is because most methods used are statistically based on decision rules determined by training samples. As the number of dimensions in the feature space increases, the number of training samples needed for image classification also increases. If the number of training samples is insufficient as is usually the case in hyperspectral imaging, statistical parameter estimation becomes inaccurate.

Different authors have proposed methods to improve the classification results. One line of research is based on statistical theory to extract important features from the original hyperspectral data prior to the classification. In this case, the objective is to remove the redundant information without sacrificing significant information. A group of these methods are compared using classification performance in [6]. They are principal component analysis [7], discriminant analysis feature extraction [8], and decision boundary feature extraction [9]. The basic idea is not new, if we concentrate only on what is relevant, the classification is a lot easier. This is the approach we have followed in this paper, but instead of designing a statistical method to do it, we propose an Artificial Neural Network architecture and training algorithm that implement a procedure to concentrate on what is relevant and ignore what is not in an automatic manner straight from the training set. In addition, this structure has proven to be very effective in discriminating different categories within hyperspectral images without any atmospheric correction. The only preprocessing the image underwent was to remove the offset through a subtraction of the average pixel value. In the following sections, we will describe the network, provide a brief overview of its training procedure and we will test its classification abilities using one of the benchmark hyperspectral processing images, the Indian Pines image obtained by AVIRIS. This spectrometer is flown on a high altitude aircraft and it acquires image data in 224 spectral bands over the spectral range 0.4 to 2.5 micrometers, at approximately 0.01 micrometers resolution, for each of 614 samples (pixels) per image line.

2 Structure of the Network and GSBP

The architecture employed in this type of networks is very similar to the classical Multiple Layer Perceptron. In fact, the activation functions of the nodes are simple sigmoids. The only difference is that each synaptic connection implements a gaussian function determined by three parameters: its center, its amplitude and its variance:

$$g(x) = A * e^{B(x-C)^2}$$

To train this structure we have developed an extension of the backpropagation algorithm, called Gaussian Synapse Backpropagation (GSBP) [10]. In what follows we will provide a brief overview of it.

First, as in any other backpropagation algorithm, we must determine what the outputs of the different layers are. We must also define the error with respect to the target values we desire and backpropagate it to the parameters determining the synaptic connections, in this case the three parameters that correspond to the gaussian function. In order to do this, we must obtain the gradients of the error with respect to each one of the parameters for each synapse. Consequently, if we define the error as the classical sum of the squares of the differences between what we desire and what we obtain:

$$E_{tot} = \sum_k \frac{1}{2}(T_k - O_k)^2$$

And as the outputs of the neurons in the hidden and output layers are:

Output: $$O_k = F\left(\sum_j h_j A_{jk} e^{B_{jk}(h_j - C_{jk})^2}\right) = F\left(O_{Net_k}\right)$$

Hidden: $$h_j = F\left(\sum_i I_i A_{ij} e^{B_{ij}(I_i - C_{ij})^2}\right) = F\left(h_{Net_j}\right)$$

If we now calculate the gradients of the error with respect to each one of the parameters of the gaussians in each layer we obtain the following equations that will be used for the modification of the gaussian corresponding to each synapses every iteration. In the ouput layer the gradient of the error with respect to $\mathbf{A_{jk}}$ is:

$$\frac{\partial E_{tot}}{\partial A_{jk}} = h_j (O_k - T_k) F'(O_{Netk})\, e^{B_{jk}(h_j - C_{jk})^2}$$

In the case of $\mathbf{B_{jk}}$**,** and $\mathbf{C_{jk}}$ we obtain:

$$\frac{\partial E_{tot}}{\partial B_{jk}} = h_j (O_k - T_k) F'(O_{Netk})\, A_{jk} (h_j - C_{jk})^2\, e^{B_{jk}(h_j - C_{jk})^2}$$

$$\frac{\partial E_{tot}}{\partial C_{jk}} = -2 h_j A_{jk} B_{jk} (O_k - T_k) F'(O_{Netk})(h_j - C_{jk})\, e^{B_{jk}(h_j - C_{jk})^2}$$

For the hidden layer we have:

$$\Theta_j = \frac{\partial E_{tot}}{\partial h_{Netj}} = \frac{\partial E_{tot}}{\partial h_j}\frac{\partial h_j}{\partial h_{Netj}} = \frac{\partial E_{tot}}{\partial h_j} F'(h_{Netj})$$

and the variation of the error with respect to $\mathbf{A_{ij}}$, $\mathbf{B_{ij}}$ and $\mathbf{C_{ij}}$ is:

$$\frac{\partial E_{tot}}{\partial A_{ij}} = I_i \Theta_j e^{B_{ij}(I_i - C_{ij})^2}$$

$$\frac{\partial E_{tot}}{\partial C_{ij}} = -2\,\Theta_j I_i A_{ij} B_{ij} (I_i - C_{ij}) \quad e^{B_{ij}(I_i - C_{ij})^2}$$

$$\frac{\partial E_{tot}}{\partial B_{ij}} = \Theta_j I_i A_{ij} (I_i - C_{ij})^2 e^{B_{ij}(I_i - C_{ij})^2}$$

3 Segmentation system

The segmentation system we have constructed is presented in figure 1. It consists of a set of Gaussian synapse based networks working in parallel over the spectral dimension of each pixel of the image. These detectors produce a detection probability surface associated with the category they have been trained for. Obviously, a pixel may be assigned a detection probability by two or more detectors. This may be due to several causes: non discriminant training sets, very similar spectra, mixtures of categories within the same pixel (take into account that depending on the altitude of the flight and the spatial resolution of the instrument a pixel may represent very large

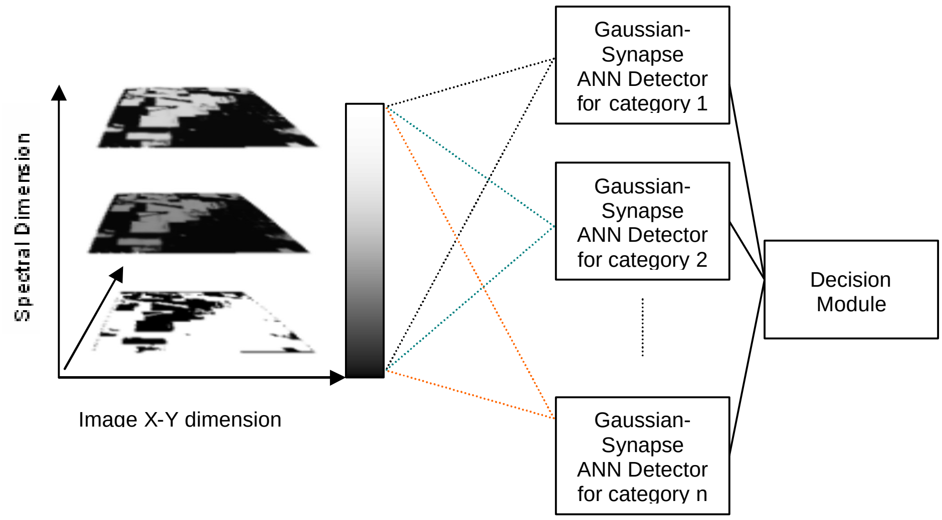

Fig. 1: Structure of the detector based segmentation system. The spectral cube is scanned in the x-y dimension and each spectrum is processed by the different detectors in parallel. The decision module constructs the final detection image.

areas areas), noise, etc. Thus, after going through the detectors, each pixel is characterized by a detection probability vector and the way this detection vector is used will depend on the application. Consequently, to decide on the final label assigned to the pixel, all the detectors send their information to a final decision module. The final decision will be made depending on the desires of the user. For instance, the decision module may be trained to choose the most likely category for the pixel or to assign combinations of detections to new categories so that the final image indicates where there is doubt or even prioritize some types of detections when searching for particular objectives such as minerals.

4 Experimental Results

The spectra used for this work correspond to the Indian Pines 1992 image obtained by the Airborne Visible/Infrared Imaging Spectrometer (AVIRIS) developed by NASA JPL which has 224 contiguous spectral channels covering a spectral region form 0.4 to 2.5 μm in 10 nm steps. It is a 145 by 145 pixel image with 220 spectral bands that contains a distribution of two-thirds of agricultural land and one-third of forest and other elements (two highways, a rail line and some houses and smaller roads). The ground truth available for this image [11] designates 16 not mutually exclusive classes. This scene has been studied by Tadjudin and Landgrebe [8][12], and also by Gualtieri et al. [13].

Instead of the atmospheric correction model used by these authors, we have started with a very simple preprocessing stage consisting in subtracting the average of the pixels in the whole image in order to eliminate offsets. The final spectra for each pixel are quite complex and misleading. As shown in figure 2 spectra corresponding to the same category may be much different than spectra from different categories. Consequently, the use of systems that incorporate the ability to obtain non linear divisions of the input space is needed. This is the context in which the Gaussian synapse networks have been used.

We have built seven networks for detecting categories in the Indian Pines image. The detectors were trained for: Soybean, Corn, Grass-Pasture, Grass-Trees, Hay-

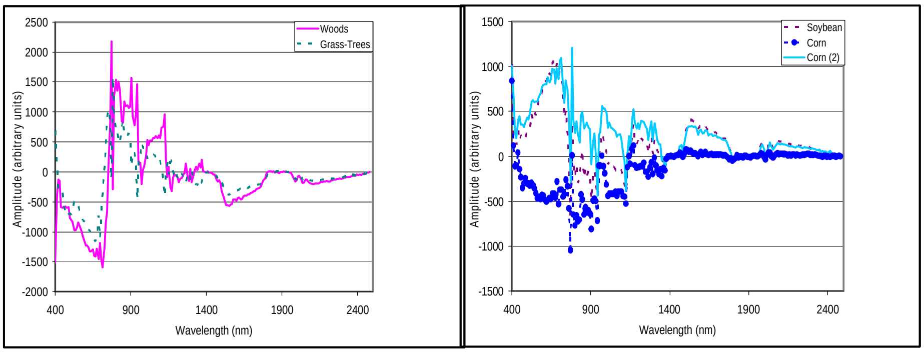

Fig. 2: In the left, two similar spectra corresponding to different categories. Right, two different spectra corresponding to the same category vs. a spectrum from a different category.

windrowed, Wheat and Woods. We group the different types of soybean and corn that were present in original image because the only difference between the types is the amount of weeds. We don't use more categories because there were insufficient number of pixels to train a network.

The training set used for all the detectors contained different numbers of pixels corresponding to the different categories (Soybean, 220; Corn, 350; GP, 220; GT, 292; HW, 320; Wheat , 130; Woods, 450). These training points were extracted from certain regions of the image, but the tests were carried out over the whole image in order to prove the generalization capabilities of the networks. In fact only less than 1% of the points of the image were used as training pixels.

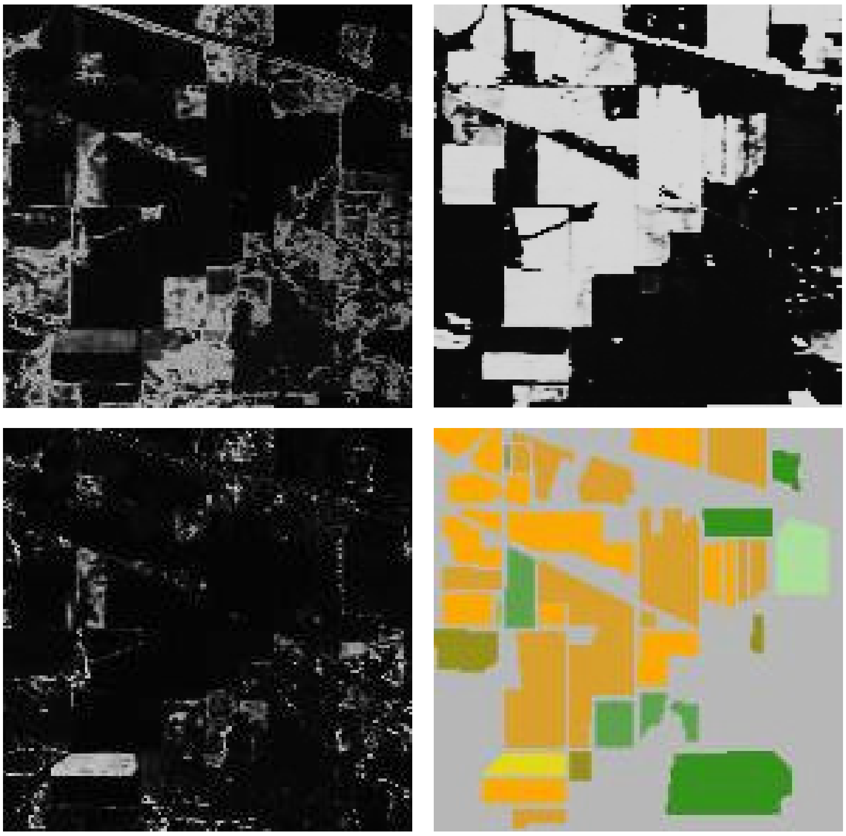

Fig. 3: Information provided by three of the detectors over the whole image. Top left: Grass pasture. Top Right: Soybean. Bottom left: Wheat. Bottom right: Ground truth.

The networks initially consist of 220 inputs, corresponding to the different spectral bands of AVIRIS. Due to the non-physical character of the pre-processing stage, unlike many other authors that manually reduce the number of spectral bands to facilitate the detector's work, we have decided to use the whole spectrum and let the network decide what is relevant. There are two hidden layers, with 18 nodes each, and one output layer corresponding to the presence or absence of the category. The training process consisted of 50 epochs in every case, with the same values for the training coefficients: 0.5 for amplitude training, 2 for variance training, and 0.5 for center training.

In figure 3 and for the purpose of providing an idea of the operation of the individual networks, we present the outputs of three of the detectors after scanning the hyperspectral image. The detectors correspond to the categories of grass pasture, soybean and wheat. There are pixels that are detected to different degrees by more than one of the detectors and in figure 4 we present the results after going through the final decision module. In this case, the figure corresponds to a maximum likelihood decision, which does not take into account any neighbourhood information. We also provide the ground-truth image in the NASA-JPL set for Indian Pines.

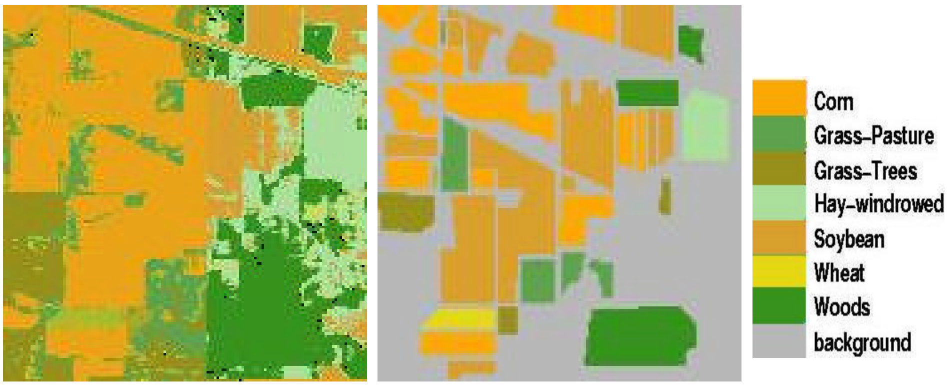

Fig. 4: From right to left. Color code of the categories, ground truth obtained in the literature for this categories and result of our networks with a final maximum likelihood decision module in segmenting the image

Several considerations may be made about these results. First of all, we must indicate that the ground truth provided had enormous areas without any labels. In the original ground truth image this areas were called background. The labelling provided by our system for these areas was very good and consistent with the indications found by other authors [8][13]. In addition, the ground truth is not detailed in the sense that there are elements within the labelled zones that were not indicated, such as roads, pathways, trees within other types of areas, etc. The system consistently detects these features. The network performs a very good classification of the whole image including all of the image regions that were no used in training at all. The only problem in the classification is the double label obtained in corn and soybean regions, where both detectors indicate the presence of their species. This is because the image was taken when the plants were only three or four weeks old and only occupied 5% of the areas labelled as soybean and corn. Corn and Soybean plants at this age are very similar from a spectroscopic point of view. Grass and wheat also present a similar problem and a double label is also obtained in some regions.

5 Conclusions

In this paper we have considered the application of Artificial Neural Networks with High-Order Gaussian Synapses and a new algorithm for training them, Gaussian Synapses Backpropagation (GSBP), to the segmentation of hyperspectral images. The structure of the segmentation system implies the use of Gaussian Synapse based networks as detectors act in parallel over the hyperspectral images providing each providing a probability of the presence of its category in each pixel. The inclusion of gaussian functions in the synapses of the networks allows them to select the appropriate information and filter out all that is irrelevant. The networks that result for each detector are much smaller than if other network paradigms were used and require a very small training set due to their great generalization capabilities. The final segmentation is made by a decision module that is trained depending on the type of segmentation desired. In the case of hyperspectral images and using a maximum likelihood decision modeule, the segmentation performed is quite good taking into account that no atmospheric modeling has been performed and, consequently, we are basically segmenting the image straight from the sensor. This makes the procedure very adequate for reducing the amount of processing required for this type of sensing strategies.

Acknowledgements

This work was supported by the MCYT of Spain (Pr. N. TIC2000-0739C0404).

References

[1] Staenz, K., Canadian Activities in Terrestrial Imaging Spectrometry, 994 Annual Report, Canada Centre for Remote Sensing, 68pp, 1995.

[2] Wiemker R., Speck A., Kulbach D., Spitzer H., Bienlein J., Unsupervised Robust Change Detection on Multispectral Imagery Using Spectral and Spatial Features. Proceedings of the Third International Airborne Remote Sensing Conference and Exhibition, Copenhagen, July 1997, vol. I, pp.640-647. ERIM, Ann Arbor 1997.

[3] Gao, B-C., and A. F. H. Goetz, Column Atmospheric Water Vapor and Vegetation Liquid Water Retrievals From Airborne Imaging Spectrometer Data, J. Geophys. Res., 95, 3549-3564, 1990.

[4] Vane, G. T., First Results of the Airborne Visible/Infrared Imaging Spectrometer (AVIRIS), SPIE, Vol 834 Imaging Spectroscopy, pp166-174, 1987

[5] Rencz A. (Editor). Manual of Remote Sensing. John Wiley and Sons, Inc. New YORK, 1999.

[6] Hsu, P.H. and Y.H. Tseng, 1999. Feature Extraction for Hyperspectral Image. Proceedings of the 20th Asian Conference on Remote Sensing, Vol. 1, pp. 405-410.

[7] Schowengerdt, R.A., 1997. Remote Sensing: Models and Methods for Image Processing, Academic Press.

[8] Tadjudin, S. and D. Landgrebe, 1998. Classification of High Dimensional Data with Limited Training Samples. PhD Thesis and School of Electrical & Computer Engineering Technical Report TR-ECE 98-8, Purdue University.

[9] Lee, C. and D. Landgrebe, 1993. Feature Extraction and Classification Algorithms for High Dimensional Data. TR-EE 93-1, Purdue University.
[10] Duro, R.J., Crespo, J.L., and Santos, J.: Training Higher Order Gaussian Synapses. LNCS, Vol. 1606 Springer-Verlag, Berlín (1999) 537-545.
[11] D. Landgrebe, Indian Pines AVIRIS Hyperspectral Reflectance Data: 92av3c, 1992. available at http://makalu.jpl.nasa.gov/locator/index.html.
[12] Tadjudin, S. and D. Landgrebe, 1998. Covariance Estimation for Limited Training Samples. Int. Geoscience and Remote Sensing Symp. Seattle, July 1998.
[13] Guatieri, J.A., Bechdol, M., Chettri, S., Robinson, J.W., Garegnani, J., Vermeulen, A. and Antonille, S. From Spectra to Cassification. Extended paper of the presentation at 1st International Symposium on Hyperspectral Analysis, Sept. 20-22, 2000, Caceres, Spain.